STUDY ON THE FRACTAL CHARACTERISTIC OF PORE THINNING EFFECT OF CONCRETE

DING XIANGQUN[1],ZHANG YICHAO[2]* , WANG FENGCHI[2],ZHOU JINGHAI[2]
[1]*School of Materials Science and Engineering, Shenyang Jianzhu University, Shenyang, China*
[2]*School of Civil Engineering, Shenyang Jianzhu University, Shenyang, China*

The fractal dimension of pore distribution of concrete is calculated based on the test of mercury intrusion porosimetry. In addition, the fractal dimension of pore distribution is used to measure and analyze the thinning effect of internal factors (such as mineral admixtures) and external factors (such as different salt ions) on pores of concrete. Results showed that the fractal dimension of pore distribution is between 1 and 2, which is greater than its topology dimension and the correlation coefficient could reach 0.98. Mineral admixtures have various extent influence of thinning effect on pores of concrete. The total porosity increases with the increasing of the fractal dimension of pore size distribution. Furthermore, the erosion experimental results and fractal analysis indicate that different kinds of compound ions solutions have different thinning effects on pores of concrete with different water-binder ratios.

Keywords: *fractal theory; mercury intrusion; fractal dimension; thinning effect*

1. Introduction

Concrete is a multi-phase (gas phase, liquid phase, solid phase) and multi-scale (micro, meso, macro) composite material system. The irregularity and uncertainty of its macro-behavior reflect the complexity of its micro-structure [1-3]. Pore properties (such as porosity, pore distribution and pore size) have important effects on physical properties (such as impermeability, frost resistance, erosion resistance) and mechanical properties (such as strength, stiffness, ductility) of concrete. As an inevitable factor of concrete, pore not only provides a transport channel for harmful ions, but also provides a reaction interface for erosion media in the process of erosion. The change of pore morphology and distribution will inevitably affect the erosion progress of harmful ions [4-6]. Literature shows that the process and mechanism of erosion of concrete by compound salt ions is complex, including the diversity of erosion products and the complexity of the transport process of harmful ions [7,8]. The effect of erosion ions on the pore is to thin the pore size in the early stage of erosion. However, the transition from specific pore size to relatively small pore size intensifies the erosion reaction theoretically. Especially for the pore size of 10-100nm, the increase of porosity will accelerate the erosion process [9-11]. In previous studies, the pore thinning effect of concrete in the early stage of erosion by compound salt ions has not been studied in depth[12]. Fractal is a means to study complex systems with self-similar and self-affine structures. Fractal theory can better characterize the pore structure characteristics of concrete, and establish the relationship between durability and pore structure of concrete[13,14].According to the characteristics of Koch curve, the pore morphology of concrete can be modified, and the boundary curve of pore can be regarded as fractal curve. Therefore, the pore characteristics described by fractal dimension are almost unchanged in the self-similar range. In this paper, based on the fractal theory and mercury intrusion porosimetry (MIP), a calculation method of fractal dimension of pore size distribution is proposed to analyze the influence of mineral admixtures on the pore structure of concrete and the thinning effect of different compound salt ions erosion on the pore structure.

2. Materials and Methods

2.1. Materials

Ordinary Portland cement (OPC), fly ash (FA), and slag(S) were used as hydraulic binders in this experiment. The chemical compositions of hydraulic binders are shown in Table 1. Fine aggregate is natural siliceous sand with fineness modulus of 2.82. Crushed stone is used as coarse aggregate. Its maximum particle size is 25mm, crushing index is 4.875%, and mud content is less than 1.0%. Naphthalene series is selected as water-reducing admixture with water reduction rate of 18%-22%.

The mix design of concrete is shown in Table 2. The specimen A, specimen B and specimen C were prepared to analyze the pore thinning effect of concrete with different contents of hydraulic binders, specimen D and specimen E were made to analyze the pore thinning effect of concrete with different contents of water-reducing admixture.

2.2. Methods

2.2.1. MIP test

All specimens were de-molded after 24 hours

*Autor corespondent/*Corresponding author*,
E-mail: zhangyichao@sjzu.edu.cn

Table 1

Chemical compositions of hydraulic binders (mass%)

	SiO_2	Al_2O_3	Fe_2O_3	CaO	MgO	SO_3	R_2O	Ignition loss
Cement	21.72	5.81	4.33	62.41	1.73	2.56	0.50	1.47
Slag	37.35	10.89	2.04	40.81	8.70	0.94	-	-
Fly ash	55.01	28.5	8.05	2.39	2.19	2.13	-	1.6

Table 2

Mix design of concrete(kg/m^3)

Specimens	Water	Cement	Slag	Fly ash	Coarse aggregates	Fine aggregates	Water-reducing admixture
A	172	400	—	100	922	851	5
B	172	350	150	—	922	851	5
C	172	350	100	50	922	851	5
D	180	315	45	90	660	1085	5
E	126	315	45	90	660	1085	7

and then cured in air with 95%RH and 20±2℃. The concrete cured for 28 days was crushed by small hammer, and the concrete particles with diameter of 3-5mm were obtained. The hydration reaction in the concrete particles was terminated by absolute ethanol. Then the treated samples were put into the oven and dried continuously at 105±2℃ for 6 hours to remove excess moisture. Then the samples were put into the expansion meter and tested by mercury intrusion porosimetry [15].

2.2.2. Compound salt ions solution erosion test

After 28 days curing, the specimen D and specimen E were immersed into three different solutions: the water solution (0), the composite salt ions solution with a concentration of 5% sodium sulfate and 3.5% sodium chloride (1), and the composite salt ions solution with a concentration of 5% sodium sulfate, 3.5% sodium chloride and 3.5% of magnesium chloride (2). The erosion tests were carried out for 90 days with temperature of 20±2℃. The specimens immersed in solutions for 90 days are shown in Fig.1. After the erosion tests, the samples were extracted from 5mm-10mm of the surface.

Fig.1 - Specimens immersed in solutions for 90 days

3. Fractal dimension of pore size distribution of concrete

MIP is an evaluation method of pore characteristics in concrete material science research. According to the functional relationship Between theamount of mercury in concrete and the pressure, the pore diameter and pore volume are calculated. In recent years, MIP is a method for testing and evaluating the pore characteristics in the scientific research of concrete materials. It calculates the diameter of the pore and the volume of the pore with different sizes according to the function relationship between the amount of mercury in the concrete and the applied pressure. Through the variation characteristics of the pore diameter and the pore volume, the fractal dimension can be directly calculated from the test data of MIP[16-18]. The volume proportion of each diameter interval is the same as the area proportion of each diameter interval, as shown below:

$$\frac{s_i}{s_t}=\frac{v_i}{v_t}=p_i \qquad (1)$$

In the formula, $s_i$and v_i are respectively the pore area and pore volume. $s_t$and v_t are respectively the total pore area and total pore volume, p_i is the volume percentage. According to fractal theory, the cumulative number N of fractal pore diameter larger than r has the following relationship with pore diameter [19]:

$$N(r)\propto\left(\frac{r}{r_{\max}}\right)^{-D} \qquad (2)$$

In the formula, r is the pore size,r_{max} is the maximal pore size, $N(r)$ is the accumulated amounts of pores, and D is fractal dimension of pore distribution.

Associated with the formula1 and formula 2, the formula3 is given as follows:

$$\sum_0^n\frac{s_t p_i}{\pi r_{mi}^2}\propto\left(\frac{r_{ni}}{r_{\max}}\right)^{-2D_f} \qquad (3)$$

In the formula,n is the number of pore diameter interval, r_{mi} and r_{ni} are the mid-value of pore diameter and the initial-value pore

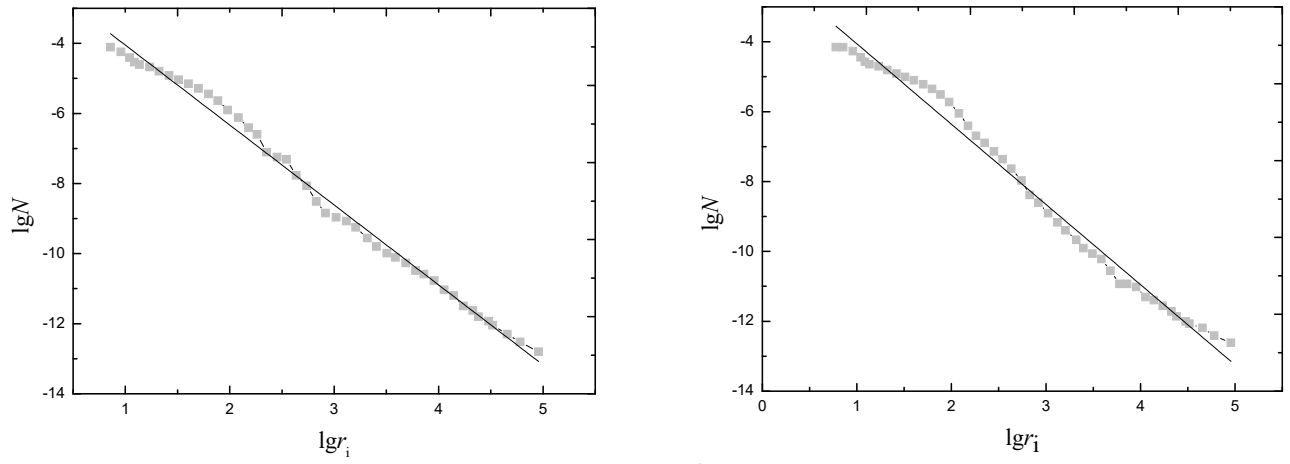

Fig. 2 - Relationship between lg*N*and lgr_i(a: Specimen A, b:Specimen B)

Table 3

Calculationresults of fractal dimension of pore size distribution

Specimens	*K*	*R*	D_f
A	2.3066	0.9891	1.1531
B	2.2964	0.9876	1.1482
C	2.2813	0.9928	1.1414
D0	2.0960	0.9887	1.0480
D1	2.1454	0.9889	1.0727
D2	2.1058	0.9899	1.0529
E0	2.0126	0.9905	1.0063
E1	2.0554	0.9936	1.0277
E2	2.0991	0.9940	1.0496

*D and E represent the concrete types, and number0, 1, 2 represent for the environment classification.

diameter respectively. Based on the data of pore size and cumulative amounts of mercury, and the measurement relationship given by formula 3, the fractal dimension of pore size distribution is calculated by taking specimen A and specimen B as examples.

Similarly,according to the above calculation method, the fractal dimension of pore size distribution of each group of specimens can be calculated. The calculation results are shown in Table 3.

It can be seen from Fig. 2 and Table 3 that the correlation coefficients of the fractal dimension of pore size distribution of concrete are all above 0.98, which shows that the calculation method is reasonable, and the pore size distribution of concrete conforms to the fractal characteristics.

And there is no obvious inflection point in the above curve. It can be concluded that this kind of fractal dimension comprehensively reflects the distribution characteristics of all pore sizes.

4. Results and discussion

4.1. Pore thinning effect of mineral material as admixtures

The pores in concrete structure can be divided into: macro pores (>10^3 nm), capillary pores (10^2nm to 10^3nm), transitional pores (10nm to10^2 nm) and gel pores (<10nm) [20]. The relationship between pore size and cumulative mercury was characterized by d*V*/dlog*D*—*D* curves of mercury intrusion porosimetry test (shown in Fig. 3), and the pore distribution was counted by pore size intervals (shown in Table 4).

Table 4

Porosity of different pore size intervals of specimens A, B and C

Specimens	Cumulative volume (ml/g)	Porosity/%				Total porosity
		＞10^3nm	10^3～10^2nm	10^2～10nm	＜10nm	
A	0.0691	16.10	31.78	49.76	2.36	14.41%
B	0.0656	18.12	32.12	45.41	4.35	12.64%
C	0.0592	13.54	32.94	50.00	3.52	7.68%

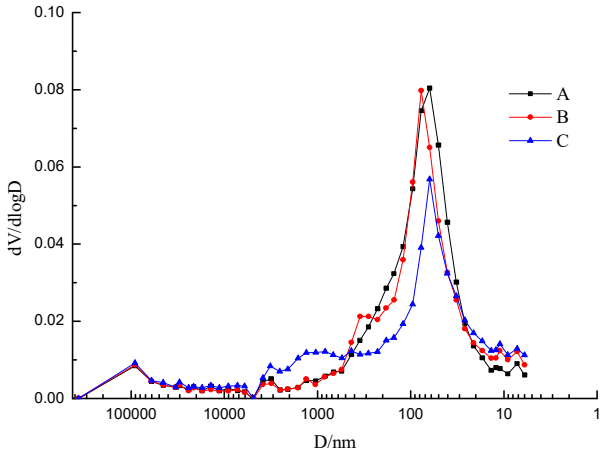

Fig. 3 - Curves of d*V*/dlog*D*—*D* of specimens A, B and C.

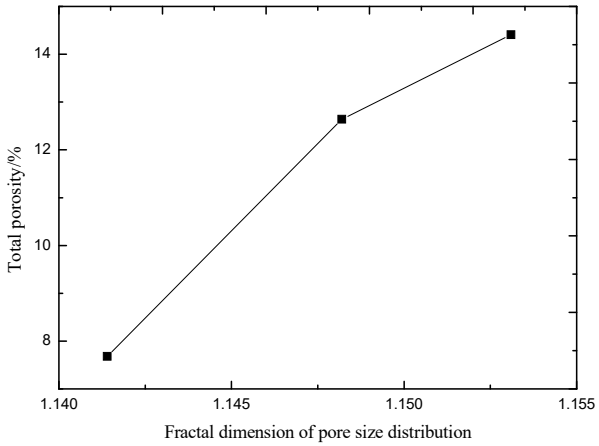

Fig. 4 - Relationship between total porosity and fractal dimension of pore size distribution.

As shown in Fig. 3 and Table 4, the total porosity of concrete mixing with fly ash is the highest, and that of concrete mixing with composite mineral materials (fly ash and slag) is the smallest, because the specific surface of fly ash is higher than that of slag.As a comprehensive index, total porosity contains information of pore volume and pore distribution, which should be affected by some parameters related to the pore classification [21].

The relationship between fractal dimension of pore size distribution and porosity is shown in Fig. 4. It is found that the total porosity increases with the increase of fractal dimension of pore distribution. The reason is the thinning effect of mineral materials on the pore of concrete. Mathematically, the pore size gradation is becoming more and more complex, and the total pore volume per unit space is also increasing.At the same water-binder ratio, the increase of porosity is not only the increase of the total number of pore, but also the degree of pore size gradation.

4.2. Pore thinning effect of erosion ions on concrete

dV/dlogD—D curves of specimen D and specimen E are plotted respectively (as shown in Fig. 5), and pore distribution was calculated according to pore size intervals (as shown in Table 5).

From Fig. 5 and Table 5, it can be seen that the porosity of pore size larger than 1000nm decreases, while that of pore size range from 100nm to 1000nm increases, and that of pore size range from 10nm to 100nm also increases. The porosity of small pore size interval presents irregular change.In 90 days, different erosion media have different characteristics in thinning the pore, but both have the characteristics of decreasing the large pore size and increasing the transition pore size. The change characteristics of porosity and fractal characteristics of pore size distribution under different erosion conditions are shown in Fig. 6 and Fig. 7, respectively.

From Fig. 6, it can be seen in specimen D that the porosity of the large pore size (>1000nm) of the sample in erosion environment 1 decreases the most comparing with the non-erosion samples, while that of the transition pore size (>10-100nm) increases the most.In erosion environment 2, the decrease range of large pore size (>1000nm) and transition pore size (>10-100nm) of specimens are lower than those of environment 1.

Compared with the non-erosion specimens with specimen E, the porosity of large pore size (>1000nm) decreased the most, and the porosity of transition pore (10-100nm) increased the most.

Table5

Porosity of different pore size intervalsof specimen D and E

Specimens	Cumulative volume (ml/g)	Porosity/%				Total porosity
		$>10^3$nm	10^3～10^2nm	10^2～10nm	<10nm	
D0	0.1303	42.52	4.61	37.10	15.73	23.21%
D1	0.1099	28.07	4.94	49.42	17.57	20.66%
D2	0.1073	40.49	7.51	41.45	10.59	19.83%
E0	0.0877	60.76	9.72	22.34	7.12	17.28%
E1	0.0754	50.74	14.23	28.87	6.23	14.13%
E2	0.084	40.22	18.63	36.39	4.70	17.23%

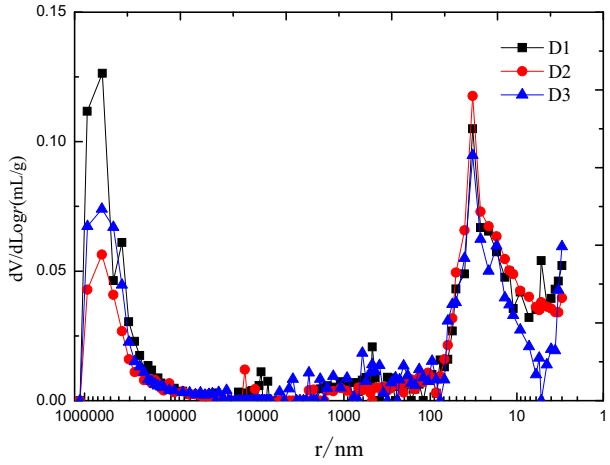

(a)

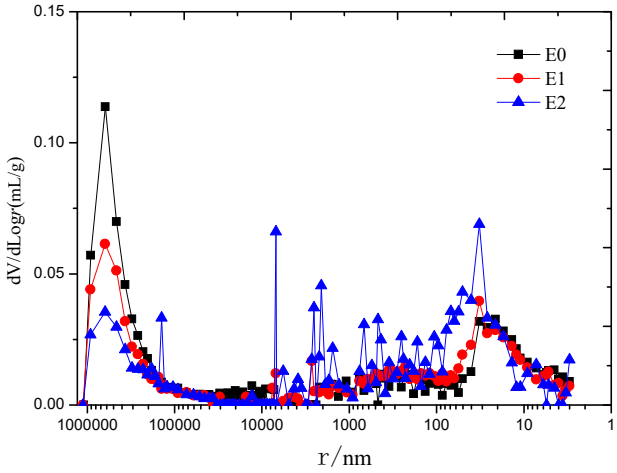

(b)

Fig. 5 - Curves of d*V*/dlog*D*—*D* (a: Specimen D, b:Specimen E)

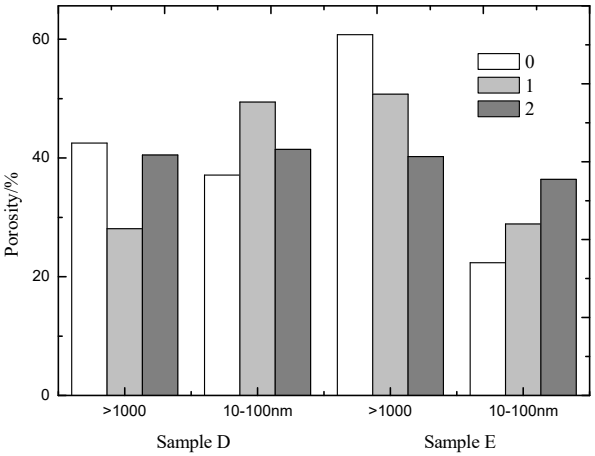

Fig. 6 - Change characteristics of porosity under different erosion conditions.

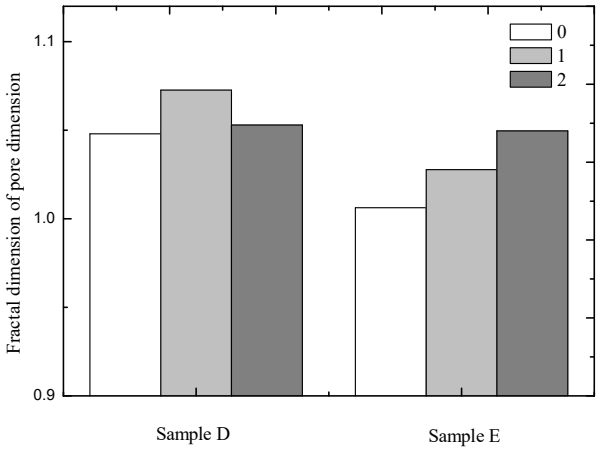

Fig. 7 - Fractal characteristics of pore size distribution under different erosion conditions

While in environment 1, the porosity of specimens with large pore size (>1000nm) and transition pore size (>10-100nm) decrease less than those in environment 2.It can be seen that in the initial stage of compound salt ions erosion, the large pore size (>1000nm) will change to the transition pore size (>10-100nm) in the erosion environment, and the erosion products will reduce the pore size.

As shown in Fig. 7, the fractal dimension of pore size distribution of concrete is increasing in erosion environment.In the early stage of erosion, chloride, sulfate and magnesium salts all thin the pore size of concrete. The formation of erosion products such as Field salt and AFt salt makes the pore move in the direction of small pore size.The erosion process itself is not a definite process. It is vulnerable to the influence of transport mechanism of erosion medium itself and pore complexity of concrete, which makes the erosion of different erosion media with different pore sizes random and makes the pore size distribution more complex. The fractal dimension of pore size distribution of specimen D in sulfate-chloride solution is larger than that in chloride-sulfate-magnesium solution, while the fractal dimension of pore size distribution of specimen E in chloride-sulfate-magnesium solution is larger than that in chloride-sulfate solution. The conclusion is consistent with the variation of porosity of large pore size (>1000nm) and transition pore (>10-100 nm).

5. Conclusions

(1) The pore size distribution of concrete conforms to fractal characteristics, and its dimension is between 1 and 2. The fractal dimension of pore size distribution of concrete with the same water-binder ratio increases with the increase of porosity, whereas decreases. Compared with fly ash, the effect of improving pore size distribution is obvious, and the effect of mixing solutions is the best.

(2) Porosity analysis in pore size range greater than 1000nm and pore size range from 10nm to 100nm shows that different kinds of compound salt ions solutions have different thinning effect under early erosion of concrete with different water-binder ratios. The thinning effect of composite chloride-sulfate solution to concrete with high water-binder ratio is higher than that of

composite chloride-sulfate-magnesium solution, while that of composite chloride-sulfate-solution to concrete with high water-binder ratio is higher. The thinning degree is higher than that of compound chloride-sulfate solution.

(3) The fractal dimension of pore size distribution can well quantify the pore thinning effect of early erosion media. The pore size distribution fractal dimension of concrete with water-binder ratio of 0.4 in sulfate-chloride salt ion solution is larger than that in chloride-sulfate-magnesium salt ion solution. The fractal dimension of pore size distribution of concrete with water-binder ratio of 0.28 in chloride-sulfate-magnesium salt ion solution is larger than that under chloride-sulfate erosion.

Funding: This research was funded by National Natural Science Foundation of China (51678374), Liaoning Province Natural Science Foundation of China (20180550092), Shenyang Science and Technology Project (17-209-9-00) and Innovation Team Project of Liaoning (LT2019011)

Conflicts of Interest: The authors declare no conflict of interest.

REFERENCES

[1] M. Tang, X. Li. The influence of multiple factors on the fractal characteristic of concrete[J]. Shenyang Jianzhu University, 2005, **21**(3), 232-235.

[2] S. Arasan, S. Akbulut, A. Samet Hasiloglu. The relationship between the fractal dimension and shape properties of particles[J]. Journal of Civil Engineering, 2011, **15**(7), 1219-1225.

[3] S. Diamond. Aspects of concrete porosity revisited[J]. Cement and Concrete Research, 1999, **29**(8), 1181-1188.

[4] Z. Jin, W. Sun, Y. Zhang, et al. Damage of concrete in sulfate and chloride solution[J]. Journal of the Chinese Ceramic Society, 2006, **34**(5), 630-635.

[5] J. Wang, Z. Sui, Z. Zhang. Test research on corrosion resistance performance of the concrete in composite salt disasters circumstance[J]. Concrete, 2013, **30**(3), 23-25.

[6] F. Weritz, D. Schaurich, A. Taffe, G. Wilsch. Effect of heterogeneity on the quantitative determination of trace elements in concrete[J]. Analytical and Bioanalytical Chemistry, 2006, **385**(2), 248-255.

[7] Z. Jin. Durability and service life prediction of concrete exposed to harsh environment in West of China[D]. Nanjing: Southeast University, 2006.

[8] R. Gao. Micro-Macro degradation regularity of sulfate attack on concrete under complex environments[D]. Beijing: Tsinghua University, 2010.

[9] L. Chen, Y. Wang, et al. Effect of aperture size on impermeability of concrete[J]. Journal of the Chinese Ceramic Society, 2005(5), 500-505.

[10] L. Chen. Effect of Aperture Size on Service Life of Concrete[J]. Journal of Wuhan University of Science and Technology, 2007(6), 50-53.

[11] M. T. Bassuoni, M. L. Nehdi. Resistance of self-consolidating concrete to ammonium sulphate attack[J]. Materials and Structures, 2012, **45**(7), 977-994.

[12] X. Liu, C. Wang, Y. Deng, F. Cao. Computation of fractal dimension on conductive path of conductiveasphalt concrete[J]. Construction and Building Materials, 2016, 115, 699-704.

[13] X. Yang, F. Wang, X. Yang, Q. Zhou. Fractal dimension in concrete and implementation for meso-simulation[J]. Construction and Building Materials, 2017, 143, 464-472.

[14] X. Yang, R. Zhang, S. Ma, X. Yang, F. Wang. Fractal dimension of concrete meso-structure based on X-raycomputed tomography[J]. Powder Technology, 2019, 350, 91-99.

[15] H. Yu, Z. Weng, W. Sun, H. Chen, J. Zhang. Influences of slag content on chlorine ion binding capacity of concrete[J]. Journal of the Chinese Ceramic Society, 2007, **35**(6), 801-806.

[16] X. Ji, S. Y. N. Chan, N. Feng. Fractal model for simulating the space-filling process of cement hydrates and fractal dimensions of pore structure of cement-based materials[J]. Cement and Concrete Research, 1997, **27**(11), 1691-1699.

[17] O. Zeng, K. Li, T. Fen-Chong, P. Dangla. Surface fractal analysis of pore structure of high-volume fly-ash cement pastes[J]. Applied Surface Science, 2010, **257**(3), 762-768.

[18] Y. Gao, K. Wu, J. Y. Jiang. Examination and modeling of fractality for pore-solid structure in cement paste: Starting from the mercury intrusion porosimetry test[J]. Construction and Building Materials, 2016, **124**, 237-243.

[19] J. Song, K. Fang, D. Liu, X. Chen. Research on fractal characteristics of phosphate slag-cement paste pore with MIP[J]. Engineering Journal of Wuhan University, 2008(12), 41-45.

[20] R. Pitchumani, B. Ramakrishnan. A fractal geometry model for evaluating permeability of porous performs used in liquid composite molding[J]. International Journal of Heat and Mass Transfer, 1999, **42**(12), 2219-2232.

[21] Z. Wu. High-Performance Concrete (in Chinese). Beijing: China Railway Press, 1999, 22-25.

****